Molecular dynamics simulation of the phase transition between calcite and $CaCO_3$-II

2009 J. Phys.: Condens. Matter 21 275403

(http://iopscience.iop.org/0953-8984/21/27/275403)

J. Phys.: Condens. Matter **21** (2009) 275403 (9pp) doi:10.1088/0953-8984/21/27/275403

Molecular dynamics simulation of the phase transition between calcite and $CaCO_3$-II

Jun Kawano, Akira Miyake[1], Norimasa Shimobayashi and Masao Kitamura

Department of Earth and Planetary Science, Faculty of Science, Kyoto University, Kyoto 606-8502, Japan

E-mail: miya@kueps.kyoto-u.ac.jp

Received 16 December 2008, in final form 20 April 2009
Published 10 June 2009
Online at stacks.iop.org/JPhysCM/21/275403

Abstract

Molecular dynamics (MD) simulation of calcium carbonate at high pressure was performed to understand the phase transition between calcite ($R\bar{3}c$) and $CaCO_3$-II ($P2_1/c$). In the 300–800 K temperature range, the transition of calcite to $CaCO_3$-II was reproduced at a pressure of around 8 GPa. This transition is of first order and reversible in the MD calculations except for runs at 300 K where a small hysteresis exists. The slope of the dP/dT curve at the phase boundary between calcite and $CaCO_3$-II is negative at 300 K and turns positive at around 600 K, which was confirmed by analyzing the enthalpy change. Just below the transition pressure, the $P2_1/c$ structure appears and its orientation switches among three positions with time, resulting in the maintenance of the $R\bar{3}c$ structure as a whole. The $P2_1/c$ structure resembles the structure of $CaCO_3$-II on an increase of temperature. It can be suggested that the existence of the $P2_1/c$ structure and the switching of its orientation just below the transition pressure are responsible for the change of the slope of the dP/dT curve at the boundary from negative to positive on an increase of temperature, because the switching increases entropy and results in an expansion of the stability field of calcite.

1. Introduction

The pressure-induced phase transformation between calcite with the space group of $R\bar{3}c$ and $CaCO_3$-II (calcite-II) with the space group of $P2_1/c$ is of interest not only for its geological applications, but also as a probe of fundamental physics. Therefore, there have been a number of investigations into this problem since the pioneering work of Bridgman (1939), who first detected a volumetric discontinuity around 1.5 GPa in the compressibility of calcite. This result led him to postulate that calcite underwent a transition to a different denser phase from aragonite within the pressure region in which aragonite is stable. Similar results were obtained later by Wang (1966, 1968), Singh and Kennedy (1974) and Vo Thanh and Lacam (1984) at room temperature, and the structure of this high-pressure metastable phase, $CaCO_3$-II, was determined using the single-crystal x-ray diffraction technique by Merrill and Bassett (1975). According to Merrill and Bassett (1975), the transition of calcite to $CaCO_3$-II results from two kinds of displacement: (1) the rotation by an angle of 11° in opposite directions of adjacent CO_3 groups along the c axis and (2) the small antiparallel displacement of Ca^{2+} ions. These displacements reduce the lattice symmetry $R\bar{3}c$ to monoclinic $P2_1/c$.

Most previous experiments (Bridgman 1939, Wang 1968, Kondo *et al* 1972) have shown a negative slope of the dP/dT curve at the phase boundary between calcite and $CaCO_3$-II at room temperature. However, a recent study by Hess *et al* (1991) reported a positive slope, so complete agreement has not been obtained. On the other hand, Kondo *et al* (1972) reported that the slope of the dP/dT curve at this phase boundary may change from negative to positive at about 250 °C. Redfern (2000) suggested that the change of slope of the dP/dT curve at this phase boundary might be reflected by a change of transition order, that is, from first order to second order upon increasing temperature. The phase relations

[1] Author to whom any correspondence should be addressed.

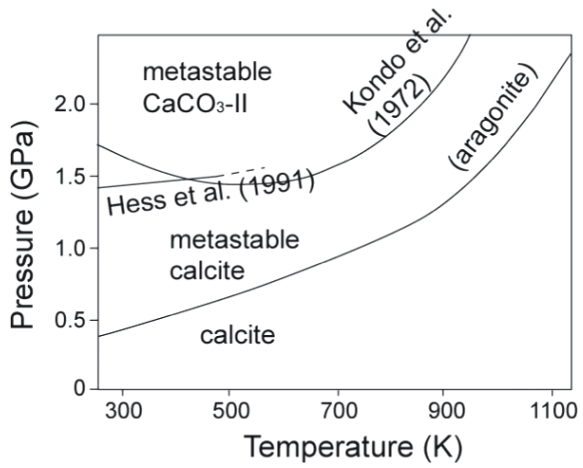

Figure 1. Phase diagrams for calcium carbonate as proposed by Kondo *et al* (1972) and Hess *et al* (1991).

proposed by Kondo *et al* (1972) are shown in figure 1, together with the experimental results of Hess *et al* (1991).

As an increase of pressure, $CaCO_3$-II was reported to transform to $CaCO_3$-III, which is followed by a further transition (e.g. Bridgman 1939, Catalli and Williams 2005). Recently the behavior of these metastable high-pressure polymorphs of calcite has received considerable attention because $CaCO_3$ has been shown to play an important role in the diamond formation at high pressure as a catalyst/solvent (Suito *et al* 2001, Catalli and Williams 2005). However, the mechanism of the transition of calcite to $CaCO_3$-II which occurs at the lowest pressure among these kinds of transitions and the slope of the dP/dT curve at the phase boundary are still ambiguous. Therefore, it is important to understand the mechanism of the transition of calcite to $CaCO_3$-II and the structure of $CaCO_3$-II.

Computer simulation is an effective technique for carrying out the structural elucidation of $CaCO_3$-II and for examining the transitional behavior between calcite and $CaCO_3$-II. Liu *et al* (2001) and Kawano *et al* (2009) studied the transitional behavior between low- and high-temperature phases of calcite using the molecular dynamics (MD) simulation technique. However, in no previous study has MD been adopted for simulation of the transition to $CaCO_3$-II and to study its structure. In the present study, we carried out MD simulations at high pressure to elucidate the mechanism of this phase transition at the atomic scale, including the problem of the slope of the dP/dT curve at the phase boundary.

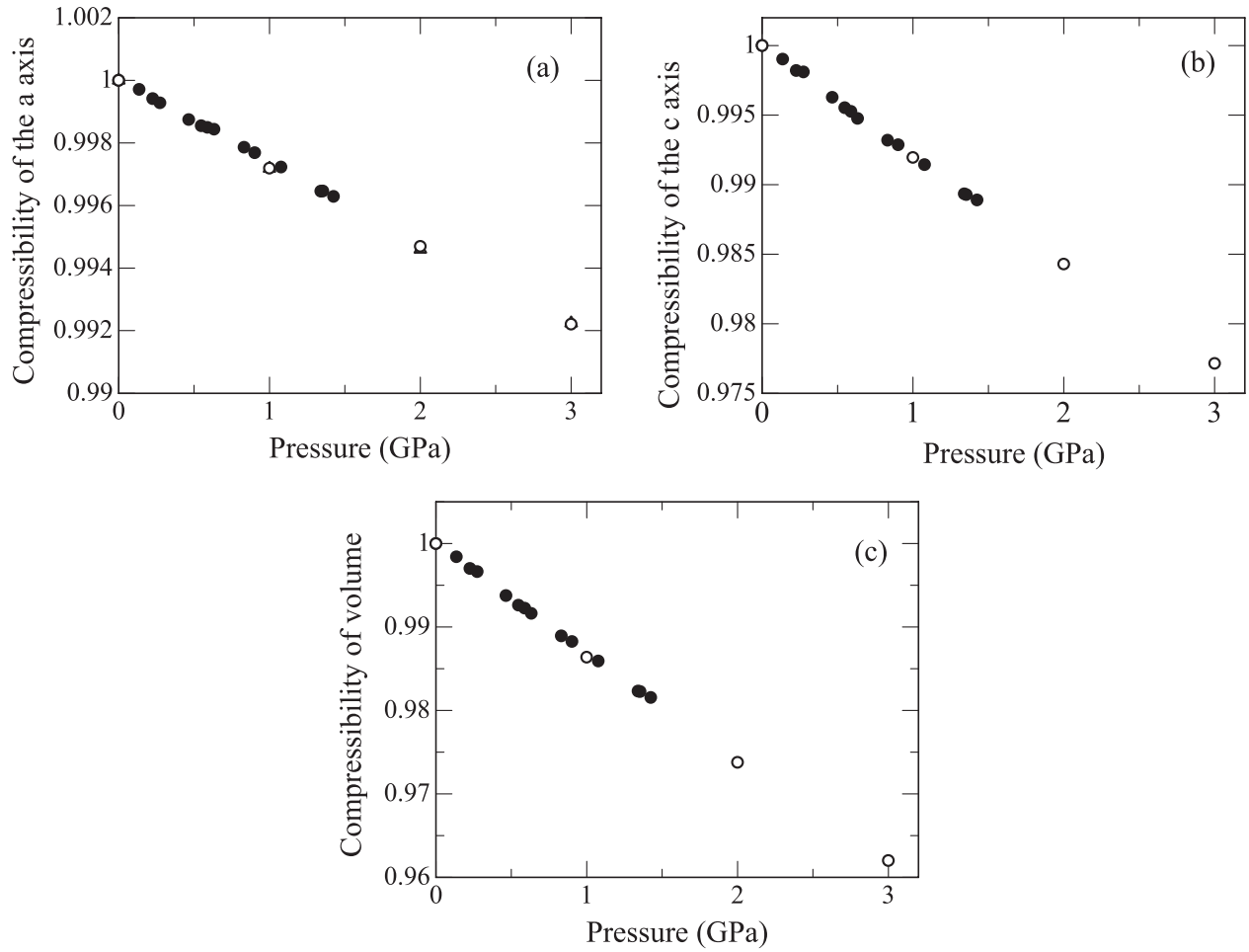

Figure 2. Pressure dependences of ((a), (b)) the compressibility of cell parameters and (c) the unit cell volume of MD simulated calcite at 300 K. The simulated values in the present study are shown by open circles (○) together with the experimental values of Redfern and Angel (1999) shown by filled circles (●).

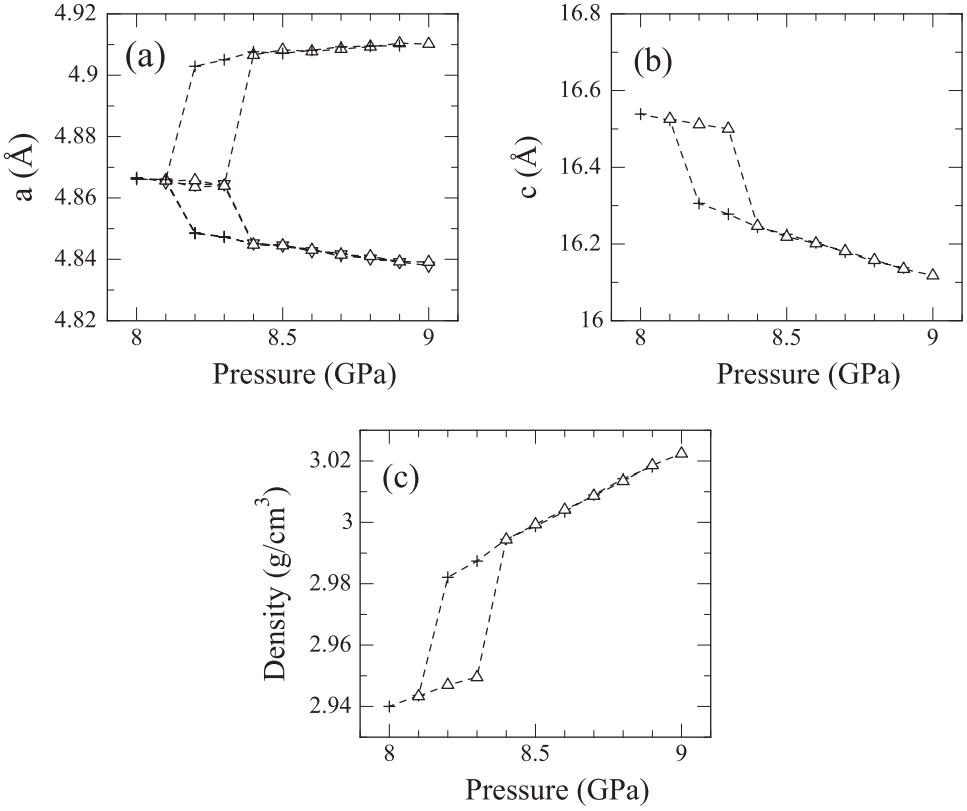

Figure 3. Pressure dependences of ((a), (b)) the a and c axes and (c) the density of MD simulated calcite between 8 and 9 GPa at 300 K. The increasing and decreasing pressure runs are shown by upright and inverted triangles (△, ▽) and crosses (+), respectively.

2. Molecular dynamics calculations

In this study, the interatomic potential model used for the MD simulation was derived by the following two procedures.

(1) The structure of calcite was optimized by using *ab initio* calculations for the bulk crystal of calcite. Then the potential energy surfaces were calculated by changing the structure parameters from the optimized structure with seven different modes, the same procedure as in Kawano *et al* (2009), which consist of three structural modes and four modes of the CO_3^{2-} ion. The structure modes are (a) stretching the hexagonal a axis while retaining the C–O bond length, (b) stretching the hexagonal c axis and (c) changing the volume while keeping the c/a ratio and C–O bond length constant. The modes of the CO_3^{2-} ion are (d) stretching all the C–O bonds while maintaining D_{3h} symmetry, which corresponds to symmetric stretching and is denoted by ν_1 in Herzberg's convention (Herzberg 1945), (e) the movement of O atoms along the c axis while maintaining the C_{3v} symmetry of the CO_3^{2-} ion, which corresponds to out-of-plane bending of the CO_3^{2-} ion (ν_2 in Herzberg's convention), (f) the movement of the CO_3^{2-} ion along the c axis while keeping the threefold axis and (g) the rotation of the CO_3^{2-} ion around the c axis while keeping the threefold axis. All quantum-mechanical computations were performed by using CRYSTAL98 code (Saunders *et al* 1999) with the Hamiltonian combining the Hartree–Fock (HF) exchange potential with the correlation potential derived by the local density approximation (LDA) based on density functional theory to reproduce the calcite structure under high-pressure conditions. In this study, the LDA correlation functional proposed by Perdew and Zunger (1981) was used.

(2) The potential energy surfaces determined from *ab initio* calculations were fitted by an interatomic potential function between two atoms and the parameter set was derived. The interatomic potential function (ϕ_{ij}) for MD calculations between two atoms (the ith and jth atoms) is given by the following equation, which is applicable to a wide variety of materials:

$$\phi_{ij}(r_{ij}) = \frac{z_i z_j e^2}{r_{ij}} + f_0(B_i + B_j)\exp\frac{A_i + A_j - r_{ij}}{B_i + B_j} - \frac{C_i C_j}{r_{ij}^6} + D_{1ij}\exp(-\beta_{1ij} r_{ij}) + D_{2ij}\exp(-\beta_{2ij} r_{ij}), \quad (1)$$

which consists of the Coulombic interaction between point charges, short range repulsion, van der Waals attraction, which is not included in the *ab initio* calculations, and Morse potential terms, where r_{ij} is the interatomic distance between the ith and jth atoms, $f_0 = 6.9511 \times 10^{-11}$ N is a constant, e is the electronic charge, z, A, B and C are the parameters for each atomic species, and D_1, D_2, β_1 and β_2 are the parameters for the C–O pair. Table 1 shows the parameter sets derived by this method.

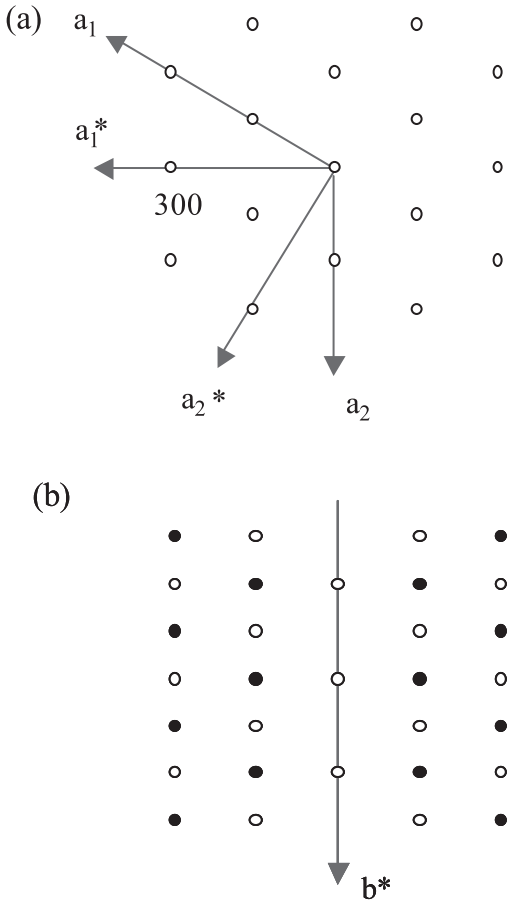

Figure 4. (a) $hk0$ zone reflections of calcite and (b) $CaCO_3$-II structure where one of the three equivalent 3/2 0 0 reflections in the hexagonal notation of calcite appears. Modified from Merrill and Bassett (1975).

MD calculations were carried out with the MD program MXDTRICL (Kawamura 1997). The Ewald method was applied for the summation of Coulombic interactions, and the equations of motions were integrated by using Verlet's algorithm with a time step of 0.5 fs. The temperatures and pressures were controlled by scaling particle velocities and simulating the cell parameters, respectively. Periodic boundary conditions were imposed by the MD basic cell. The present MD calculations were performed by using an MD cell composed of 72 crystallographic unit cells of calcite ($a_{MD} = 6a, c_{MD} = 2c$) in a hexagonal setting containing 2160 atoms. The structure obtained by Wyckoff (1963) was adopted as the initial structure. First, the structure was relaxed to the equilibrium state by annealing at 300 K for at least 40 000 steps (20 ps). After that, the temperature was increased to the required value, 300–900 K, at intervals of 100 K, while keeping the pressure constant (1 atm). The pressure-increasing runs were carried out by using structures calculated at 1 atm, which were confirmed to be low-temperature calcite. In these runs, the pressure was increased while holding the temperature constant. The pressure-decreasing runs were also carried out with the high-pressure structure as the initial state. The diffracted intensity was calculated from the structure factor that was obtained directly from the MD simulated atomic positions by using a program developed by Miyake *et al* (1998).

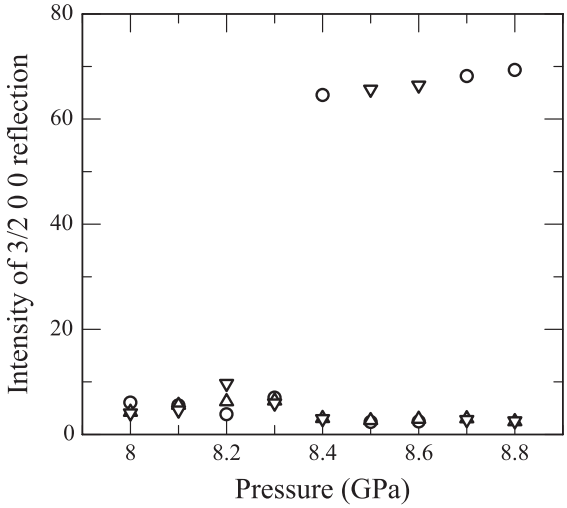

Figure 5. Pressure dependence of the intensities of three equivalent 3/2 0 0 reflections in the $R\bar{3}c$ structure at 300 K. Among the three equivalent 3/2 0 0 reflections indicated by open circles and upright and inverted triangles at low pressure, only one reflection along one direction appears at high pressure.

Table 1. Parameter sets for the interatomic potential function (equation (1)), which were determined by fitting the energy surfaces calculated with *ab initio* methods.

Atom	Z (e)	A (Å)	B (Å)	C (kcal$^{1/2}$ Å^3 mol$^{-1/2}$)
O	−0.976	1.8310	0.1752	20.0888
C	1.056	0.5913	0.0533	0.000
Ca	1.872	1.5059	0.0898	7.9400

Atomic pair	D_1 (kJ mol^{-1})	β_1 (Å^{-1})	D_2 (kJ mol^{-1})	β_2 (Å^{-1})
O–C	38 843.41	5.509	−3293.856	2.503

The relaxed structure at 300 K and 1 atm is summarized in table 2, which shows very good agreement with experimental data. The lattice constants of the simulated structure, a and c axis lengths and the unit cell volume, change with increasing pressure at 300 K. Their pressure dependence between 1 atm and 3 GPa is shown as compressibility in figure 2. The experimental results that are also plotted in this figure were obtained by the single-crystal x-ray diffraction method (Redfern and Angel 1999) only up to 1.5 GPa, where calcite transforms to $CaCO_3$-II. Figure 2 shows that the compressibility of the cell parameters can be reproduced perfectly in this pressure range with this parameter set. This result reveals that the present interatomic potential parameter is highly effective for calculations at high pressure.

3. Results and discussions

3.1. Phase transition from calcite to $CaCO_3$-II at 300 K

The results of the simulation at high pressures between 8 and 9 GPa at 300 K (figure 3) show the discontinuous changes

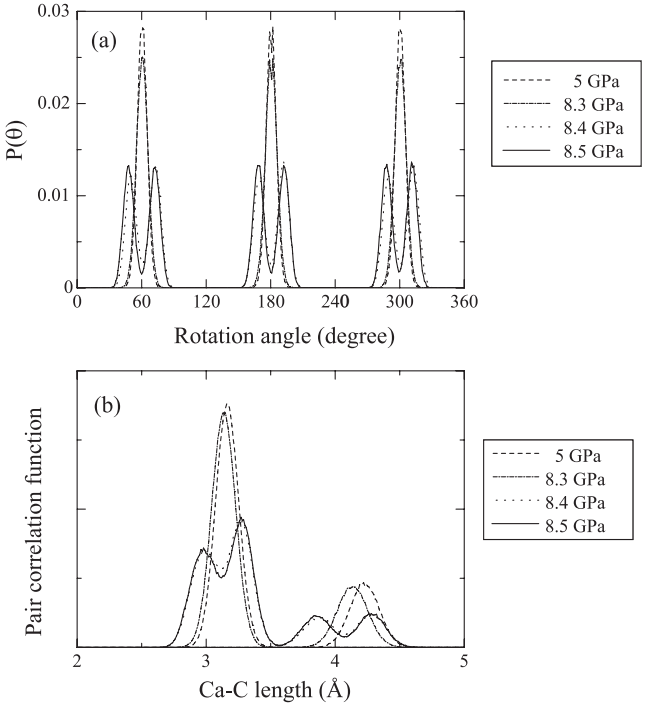

Figure 6. Pressure dependence of (a) the probability distribution function $P(\theta)$ for the angle θ, between the a axis and the C–O bonds in the same plane at 300 K, and (b) the pair correlation function for Ca–C pairs at 300 K.

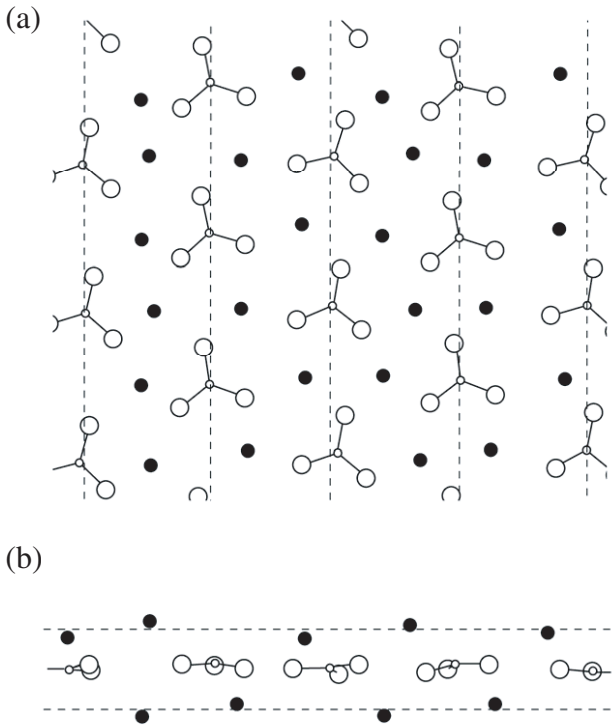

Figure 7. A 'snapshot' of the simulated $CaCO_3$-II structure calculated at 300 K and 9 GPa, (a) view looking down and (b) normal to the c axis in calcite. Ca atoms are represented by closed circles, O atoms are large open circles and C atoms are small open circles. Dashed lines show the direction of the calcite axes. CO_3 groups rotate about $+10$ or $-10°$, and Ca atoms in a layer are displaced by turns near to and far from the adjacent CO_3 layer.

Table 2. The crystallographic parameters of relaxed calcite structure at 300 K and 1 atm, obtained by the present MD calculations and from the experimental data of Effenberger *et al* (1981).

	MD	Obs.
a_h (Å)	4.951	4.9896
c_h (Å)	17.514	17.061
V (Å^3)	371.79	367.846
ρ (g cm^{-3})	2.68	2.71
C–O (Å)	1.2583	1.2813

of the length of the c axis and the density, and that the three equivalent a axes split into two equivalent short axes and one long axis at around 8.4 GPa. This transition can be characterized as a compression in one direction.

Merrill and Bassett (1975) suggested that the transition from calcite to $CaCO_3$-II accompanies the symmetry change from rhombohedral $R\bar{3}c$ to monoclinic $P2_1/c$, and that only one of the three equivalent 3/2 0 0 reflections in the hexagonal notation of calcite would appear in the structure of $CaCO_3$-II (figure 4). Figure 5 shows the pressure dependence of the intensities of three equivalent 3/2 0 0 reflections for the pressure-increasing runs at 300 K. Only one of these reflections has a substantial intensity at the pressure where the cell parameters change discontinuously, indicating that the phase transition from rhombohedral $R\bar{3}c$ to monoclinic $P2_1/c$ is reproduced in the present MD simulation.

The orientational angular distributions of C–O bonds from the a axis, $P(\theta)$, are shown in figure 6(a). This figure shows that the O atoms vibrate at the equilibrium sites of the $R\bar{3}c$ structure below 8.3 GPa. Above 8.4 GPa, the positions of the O atoms split into two, each of which is rotated by either about $+10°$, or about $-10°$, around the threefold axis. Figure 6(b) shows the pair correlation function for Ca–C at 300 K calculated between 2 and 5 Å. Below 8.3 GPa, there are two single peaks at around 3.1 and 4.2 Å, while above 8.4 GPa each single peak splits into two.

One of the 'snapshots' of the atomic arrangement of the high-pressure phase obtained in the calculation at 300 K and 9 GPa is shown in figure 7. The atomic arrangement of this high-pressure phase is the same as that of the structure obtained by Merrill and Bassett (1975). CO_3 groups also rotate by either about $+10°$, or about $-10°$, around the threefold axis as shown in figure 7; in relation to the rotation of CO_3 groups, Ca atoms in a layer are displaced by turns near to and far from the adjacent CO_3 layer. This behavior is responsible for the splits of each single peak into a doublet in the Ca–C pair correlation function (figure 6(b)). These displacements of the CO_3 groups and Ca ions characterize the structure of $CaCO_3$-II.

Therefore, we conclude that the transition between calcite and $CaCO_3$-II is reproduced basically in the present MD simulations and the transition pressure is around 8.3 GPa at 300 K, while the transition pressure is higher than those obtained in previous experimental studies.

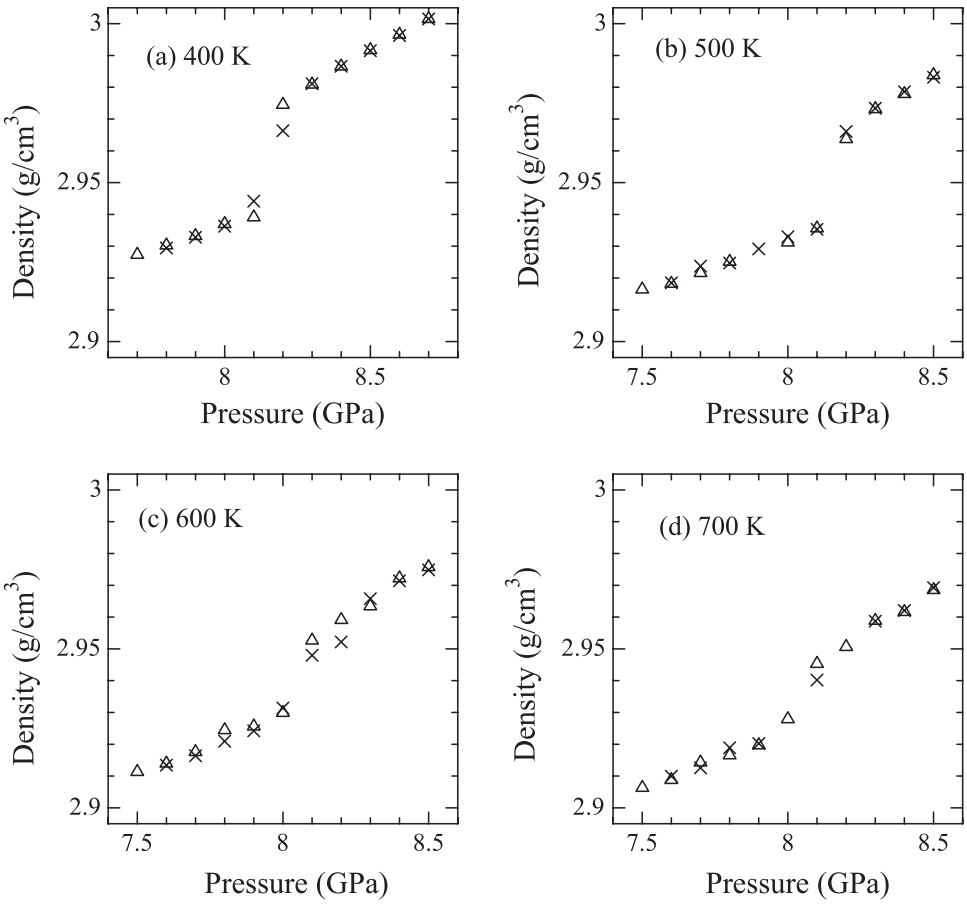

Figure 8. Pressure dependences of the density of MD simulated calcite between 8.5 and 9.5 GPa at (a) 400 K, (b) 500 K, (c) 600 K and (d) 700 K. Results from the pressure-increasing runs are shown as upright triangles (△) and values from the pressure-decreasing runs are shown as crosses (+).

3.2. Phase relation between calcite and $CaCO_3$-II

Both increasing and decreasing pressure runs were also carried out at elevated temperatures. The pressure dependences of the density in a temperature range from 400 to 700 K are shown in figure 8. Discontinuous changes of the density are also observed at the transition pressures and the magnitude of the changes becomes smaller on an increase of temperature. From 400 to 700 K the discontinuities occur at the same pressure for both the increasing and decreasing pressure runs without hysteresis, while a small hysteresis is observed at 300 K (figure 3). Therefore, this transition is of first order and nearly reversible. This is consistent with previous experimental results (e.g. Merrill 1974).

The phases that appear under various P–T conditions in the present simulation are plotted in figure 9. In addition to the structures of calcite and $CaCO_3$-II, a structure including C atoms surrounded by four O atoms appears as an increase of pressure at high temperatures. Such coordination, however, is not chemically permissible in a real structure and the corresponding phase is shown by a cross (×) in figure 9. The phase boundary between calcite and $CaCO_3$-II on the pressure where the discontinuity in the cell parameters is observed at each temperature is not straight but curved. In order to confirm the change of the slope of the dP/dT curve at the phase boundary in figure 9, the difference between the enthalpies of calcite and $CaCO_3$-II ($\Delta H_{\text{calcite}}^{\text{CaCO}_3\text{–II}}$) was calculated. Because the difference in the Gibbs free energy between the two phases ($\Delta G_{\text{calcite}}^{\text{CaCO}_3\text{–II}} = \Delta H_{\text{calcite}}^{\text{CaCO}_3\text{–II}} - T\Delta S_{\text{calcite}}^{\text{CaCO}_3\text{–II}}$) should be equal to zero at the phase boundary, the enthalpy change at the phase boundary is expressed as

$$\Delta H_{\text{calcite}}^{\text{CaCO}_3\text{–II}} = T\Delta S_{\text{calcite}}^{\text{CaCO}_3\text{–II}}. \tag{2}$$

Substituting equation (2) into the Clausius–Clapeyron equation

$$\frac{dP}{dT} = \frac{\Delta S}{\Delta V}, \tag{3}$$

the slope of the dP/dT curve at the phase boundary is expressed as follows:

$$\frac{dP}{dT} = \frac{\Delta H_{\text{calcite}}^{\text{CaCO}_3\text{–II}}}{T\Delta V_{\text{calcite}}^{\text{CaCO}_3\text{–II}}}. \tag{4}$$

Therefore, the enthalpy and volume differences between the two phases lead to the gradient of the phase boundary.

For example, the pressure dependences of the enthalpy and volume per mol at 500 K are shown in figure 10. Linear dependences of the enthalpies of calcite and $CaCO_3$-II upon pressure are calculated. There is only a small difference (about

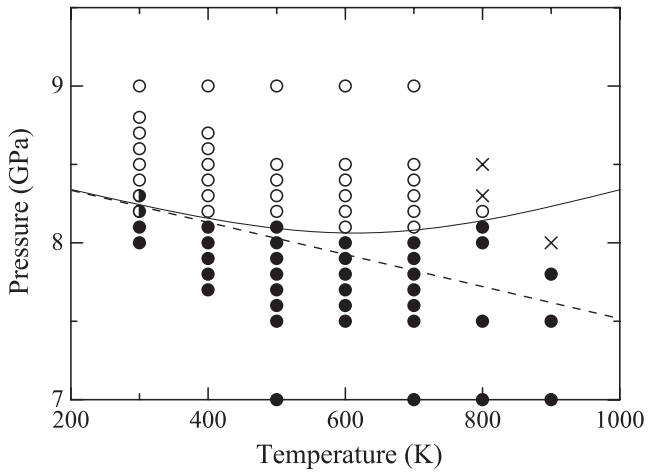

Figure 9. P–T diagram for the appearance of the phase at each calculation condition. Calcite is represented by filled circles (●), $CaCO_3$-II by open circles (○), the transition between calcite and $CaCO_3$-II with the hysteresis by half-filled circles (◑) and the structure including C atoms surrounded by four O atoms by crosses (×). The solid line is the phase boundary between calcite and $CaCO_3$-II. The slope of the phase boundary changes from negative to positive at around 700 K. A hypothetical phase boundary under the condition where the $P2_1/c$ structure do not appear just below the transition pressure at high temperature is drawn by a dashed line.

60 J mol^{-1}) between the two lines at the transition pressure of 8.15 GPa. The volume difference, $\Delta V_{\text{calcite}}^{\text{CaCO}_3-\text{II}}$, calculated from the cell parameters is about -0.3 cm^3 mol^{-1}. Therefore, the gradient of the phase boundary is about -4.0×10^{-4} GPa K^{-1} at 500 K. This value is in very good agreement with the results shown in figure 9. In the same manner, the gradients of the phase boundary $\mathrm{d}P/\mathrm{d}T$ at other temperatures from 300 to 700 K were calculated and summarized in table 3 with the values of $\Delta H_{\text{calcite}}^{\text{CaCO}_3-\text{II}}$, $\Delta S_{\text{calcite}}^{\text{CaCO}_3-\text{II}}$ and $\Delta V_{\text{calcite}}^{\text{CaCO}_3-\text{II}}$ at each temperature. These results show that, on an increase of temperature, the gradient increases from -1.3×10^{-3} GPa K^{-1} at 300 K to almost zero at 600 K and slightly positive at 700 K. This tendency is consistent with that observed in figure 9. While the gradient at 800 K could not be calculated because the $CaCO_3$-II structure appeared at only one pressure (8.2 GPa), the gradient of the $\mathrm{d}P/\mathrm{d}T$ curve may change to positive at around 600 K. This behavior of the phase boundary is consistent with the phase diagrams of Kondo *et al* (1972) and Redfern (2000), while it contradicts the result of Hess *et al* (1991).

3.3. Transition mechanism between calcite and $CaCO_3$-II

To discuss the transition mechanism, the time dependence of the intensities of the 3/2 0 0 reflections is considered. Figure 11 shows the change of three equivalent 3/2 0 0 reflections at 300 K and at 8.1, 8.3 and 8.4 GPa. Sufficiently below the transition pressure, for example at 8.1 GPa, all of the intensities of the three reflections are equivalent and have almost zero value, indicating the $R\bar{3}c$ structure (figure 11(a)). Above 8.4 GPa only one reflection among the three has significantly stronger intensity than the other two, indicating the $P2_1/c$ structure (figure 11(c)). In an intermediate pressure between 8.1 and 8.4 GPa, the intensity of one of the three equivalent reflections becomes a little stronger than those of

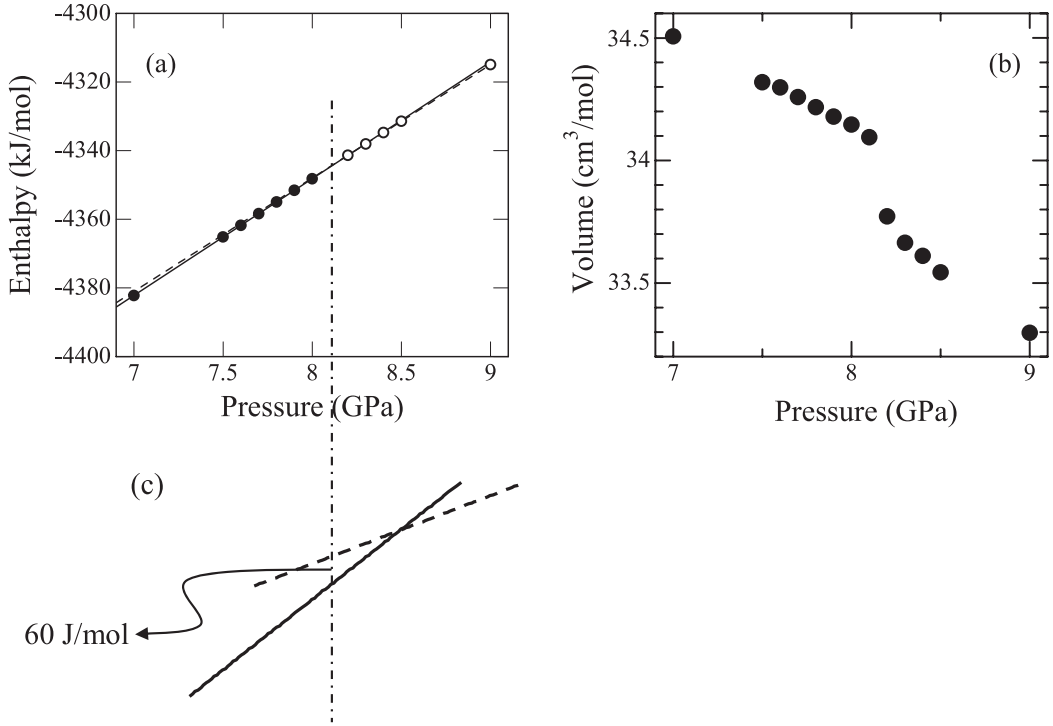

Figure 10. Pressure dependences of (a) the enthalpy and (b) the molar volume at 500 K, obtained by the present MD calculations. In (a), the enthalpies of calcite are shown by filled circles (●) and the least-squares fit by a solid line. The enthalpies of $CaCO_3$-II are shown by open circles (○) and a dashed line. (c) Schematic drawing of the enthalpy change around the transition pressure.

Table 3. The calculated slope dP/dT of the phase boundary between calcite and $CaCO_3$-II at each temperature.

T (K)	ΔH (J mol^{-1})	ΔS (J mol^{-1} K^{-1})	ΔV (cm^3 mol^{-1})	dP/dT ($\times 10^{-3}$ GPa K^{-1})
300	159.08	0.530	−0.40	−1.326
400	124.83	0.312	−0.45	−0.693
500	60.29	0.121	−0.30	−0.402
600	12.49	0.021	−0.20	−0.104
700	−3.05	−0.004	−0.20	0.022

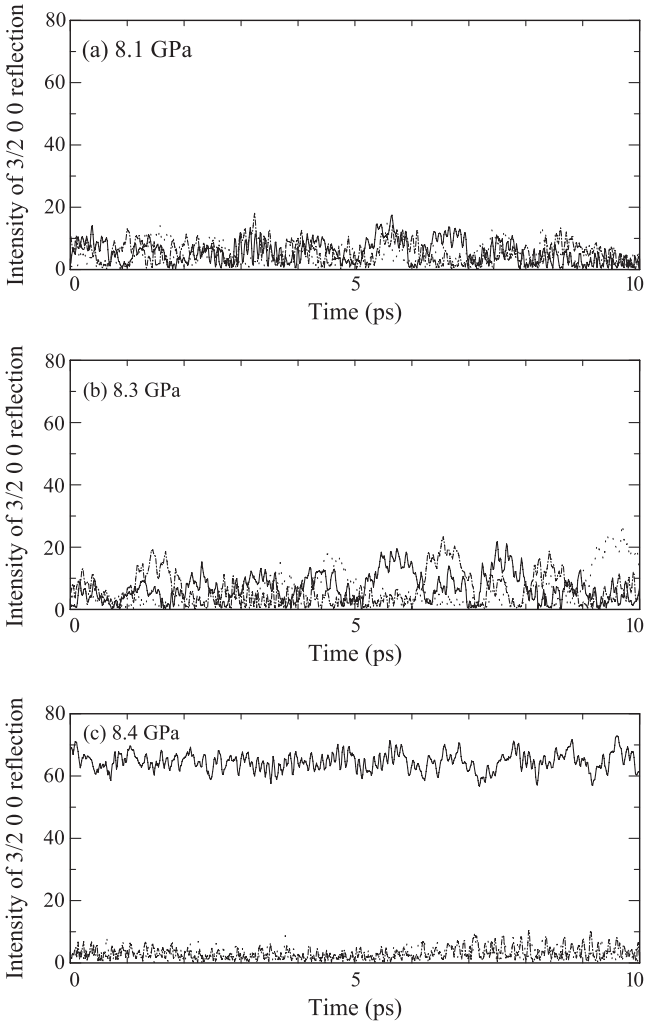

Figure 11. Time dependences of the intensities of three equivalent 3/2 0 0 reflections of calcite for pressure-decreasing runs at 300 K and at (a) 8.1 GPa, (b) 8.3 GPa and (c) 8.4 GPa. The solid, dashed–dotted and dotted lines show the three equivalent a axes in the hexagonal notation of calcite.

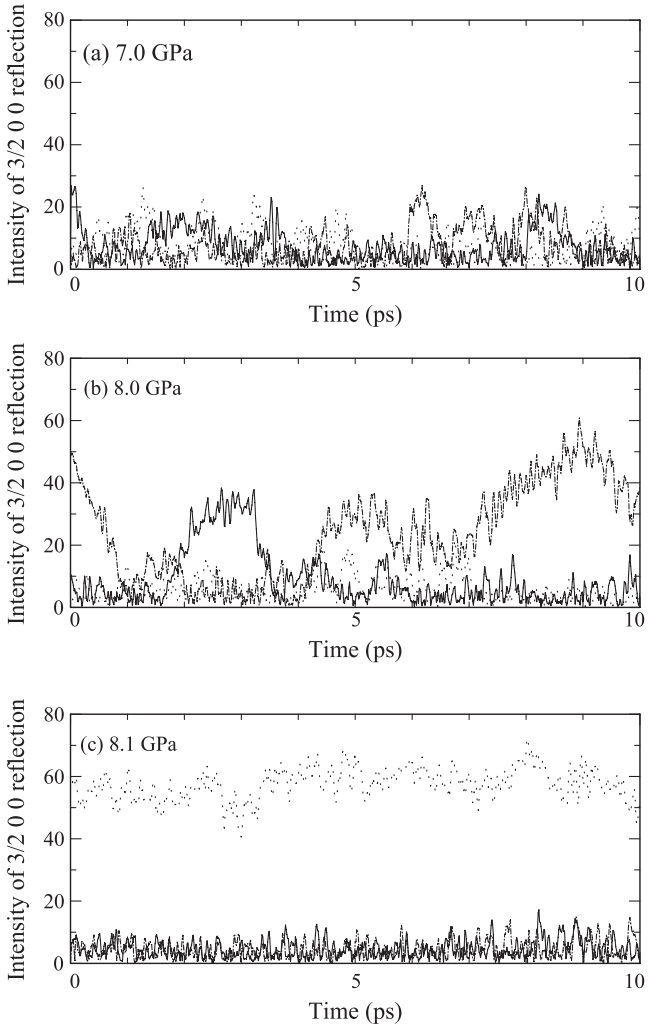

Figure 12. Time dependences of the intensities of three equivalent 3/2 0 0 reflections of calcite for pressure-increasing runs at 700 K and (a) 7.0 GPa, (b) 8.0 GPa and (c) 8.1 GPa. The solid, dashed–dotted and dotted lines show the three equivalent a axes in the hexagonal notation of calcite.

the others in short periods of the MD calculations. The changes of the intensities at 8.3 GPa are shown in figure 11(b). The direction of the reflection with the strongest intensity changes with time; the b3 direction in the period of 4.3–4.7 ps, b1 in 5.3–6.0, b2 in 6.2–7.0, b1 in 7.2–8.0, b2 in 8.0–8.6 and b3 in 9.2–10. This behavior can be interpreted as that the $P2_1/c$ structure appears in each period and the orientation of the structure (e.g. direction of the b^* axis of the $P2_1/c$ structure; see figure 4) switches among three positions with time. Therefore, the $R\bar{3}c$ structure is considered to be still maintained as a whole in the intermediate pressure range.

The time dependences of the intensities of the three equivalent reflections at 700 K are shown in figure 12 and are basically the same as those at 300 K (figure 11). Significantly below the transition pressure, all intensities of the three equivalent reflections are almost zero, indicating that the symmetry is $R\bar{3}c$ (figure 12(a)). Above the transition pressure, the intensity in one direction becomes stronger than in the

other directions and the symmetry is $P2_1/c$ (figure 12(c)). Just below the transition pressure, the intensity of one of the three equivalent reflections does not equal the others in short periods, similar to the MD simulation at 300 K. The intensity of the one reflection is also stronger than at 300 K (figures 11 and 12(b)). This means that the structure appearing for short periods at 700 K is more similar to the $P2_1/c$ structure of $CaCO_3$-II than that at 300 K. The time intervals for the switching of the orientations at 700 K are longer than those at 300 K, indicating that the structure at 700 K may be more stable than that at 300 K. Therefore, the $P2_1/c$ structure appearing just below the transition pressure resembles the structure of $CaCO_3$-II on an increase of temperature. The existence of the $P2_1/c$ structure as a precursor for the transition to $CaCO_3$-II at high temperature implies that the order of the transition approaches second order as the temperature increases to 700 K. This implication is supported by the fact that the change of the cell parameters becomes continuous as an increase of temperature (figure 8). By using Landau theory, Hatch and Merrill (1981) suggested that this transition is continuous, although no experiment has shown any evidence of such a continuous transition. The present results support the suggestion by Hatch and Merrill (1981).

The present MD calculations show that the slope of the dP/dT curve changes from negative to positive at around 600 K (figure 9). This change of the slope of the dP/dT curve must be related to the existence of the $P2_1/c$ structure and the switching among the three orientations just below the transition pressure, because the switching causes an increase of entropy, resulting in an expansion of the stability field of calcite. When no switching of the orientations occurs, the slope would not be changed so much in the whole pressure range as schematically shown in figure 9. It can be concluded that the existence of the $P2_1/c$ structure and the switching of its orientation just below the transition pressure are responsible for the change of the slope of the dP/dT curve at the boundary from negative to positive as an increase of temperature.

Acknowledgments

We thank K Kawamura for constructive suggestions. This work was supported by a Grant-in-Aid for Scientific Research from the Japanese Ministry of Education, Science, Sports, and Culture.

References

Bridgman P W 1939 The high pressure behavior of miscellaneous minerals *Am. J. Sci.* **237** 7–18

Catalli K and Williams Q 2005 A high-pressure phase transition of $CaCO_3$-III *Am. Mineral.* **90** 1679–82

Effenberger H, Mereiter K and Zemann J 1981 Crystal structure refinements of magnesite, calcite, rhodochrosite, siderite, smithsonite and dolomite, with discussion of some aspects of the stereochemistry of calcite-type carbonates *Z. Kristallogr.* **156** 233–43

Hatch D M and Merrill L 1981 Landau description of the calcite–$CaCO_3$(II) phase transition *Phys. Rev.* B **23** 368–74

Herzberg G 1945 *Infrared and Raman Spectra of Polyatomic Molecules* (New York: Van Nostrand-Reinhold)

Hess N J, Ghose S and Exarhos G J 1991 Raman spectroscopy at simultaneous high pressure and temperature: phase relations of $CaCO_3$ and the lattice dynamics of the calcite ↔ $CaCO_3$(II) phase transition *Recent Trends in High Pressure Research; Proc. 13th AIRAPT Int. Conf. on High Pressure Science and Technology* ed A K Singh (New Delhi: Oxford & IBH Publishing Co. Pvt) pp 236–41

Kawamura K 1997 *MXDTRICL* Japan Chemical Program Exchange, #77

Kawano J, Miyake A, Shimobayashi N and Kitamura M 2009 Molecular dynamics simulation of the rotational order–disorder transition in calcite *J. Phys.: Condens. Matter* **21** 095406

Kondo S, Suito K and Matsushima S 1972 Ultrasonic observation of calcite I–II inversion to 700 °C *J. Phys. Earth* **20** 245–50

Liu J, Duan C-G, Ossowski M M, Mei W N, Smith R W and Hardy J R 2001 Simulation of structural phase transition in $NaNO_3$ and $CaCO_3$ *Phys. Chem. Miner.* **28** 586–90

Merrill L 1974 A soft mode mechanism for the displacive calcite–$CaCO_3$(II) phase transformation at 1.5 GPa *Proc. 4th Int. Conf. on High Pressure (Kyoto)* pp 389–92

Merrill L and Bassett W A 1975 The crystal structure of $CaCO_3$ (II), a high-pressure metastable phase of calcium carbonate *Acta Crystallogr.* B **31** 343–9

Miyake A, Hasegawa H, Kawamura K and Kitamura M 1998 Symmetry and its change in a reciprocal space of a quartz crystal simulated by molecular dynamics *Acta Crystallogr.* A **54** 330–7

Perdew J P and Zunger A 1981 Self-interaction correction to density-functional approximations for many-electron systems *Phys. Rev.* B **23** 5048–79

Redfern A T S 2000 Structural variations in carbonate *High-Temperature and High-Pressure Crystal Chemistry, Reviews in Mineralogy and Geochemistry* vol 41, ed M H Hazen and R T Downs (Washington, DC: Mineralogical Society of America) pp 289–308

Redfern A T S and Angel R J 1999 High-pressure behaviour and equation of state of calcite, $CaCO_3$ *Contrib. Mineral. Petrol.* **134** 102–6

Saunders V R, Dovesi R, Roetti C, Causá M, Harrison N M, Orlando R and Zilcovich-Wilson C M 1999 *CRYSTAL98 User's Manual* University of Torino, Torino

Singh A K and Kennedy G C 1974 Compression of calcite to 40 kbar *J. Geophys. Res.* **79** 2615–22

Suito K, Namba J, Horikawam T, Taniguchi Y, Sakurai N, Kobayashi M, Onodera A, Shimomura O and Kikegawa T 2001 Phase relations of $CaCO_3$ at high pressure and high temperature *Am. Mineral.* **86** 997–1002

Vo Thanh D and Lacam A 1984 Experimental study of the elasticity of single crystalline calcite under high pressure (the calcite I–calcite II transition at 14.6 kbar) *Phys. Earth Planet. Inter.* **34** 195–203

Wang C 1966 Velocity of compressional waves in limestones, marbles, and a single crystal of calcite to 20 kbars *J. Geophys. Res.* **71** 3543–7

Wang C 1968 Ultrasonic study of phase transition in calcite to 20 kbars and 180 °C *J. Geophys. Res.* **73** 3937–44

Wyckoff R W G 1963 *Crystal Structures* (New York: Wiley)